Appl. Phys. B 85, 85–88 (2006)
DOI: 10.1007/s00340-006-2402-z

Applied Physics B
Lasers and Optics

J.-H. HAN[1,2,✉]
Z. LHEE[2]
S.-W. PARK[3]

Characterization of loss-coupled 1550 nm DFB lasers for microwave optical links

[1] Department of Electrical and Computer Engineering, Johns Hopkins University, 3400 North Charles Street, Baltimore, MD 21218, USA
[2] Telecommunications Research Laboratory, LS Cable Ltd., 555 Hogyedong, Dognangu, Anyang, 431-080, Republic of Korea
[3] Optical Communications Research Center, Electronics and Telecommunications Research Institute, 1110-6 Oryong-dong, Buk-gu, Gwangju, 500-480, Republic of Korea

Received: 19 December 2005/Revised version: 5 July 2006
Published online: 3 August 2006 •

ABSTRACT A loss-coupled 1550 nm distributed feedback (DFB) laser diode with automatically buried absorptive InAsP layer for the application to radio-over-fiber network was experimentally investigated where the automatically buried layer in the epitaxial growth reduced the process steps in loss-coupled DFB laser fabrication. It showed linearity in electro-optical conversion characteristics with reduced third order intermodulation distortion of −70 dBc which is comparable to the previous results of DFB lasers as the optical power increases to 5 mW under two-tone test at 1.8 GHz bands.

PACS 42.55.Px; 42.79.Sz

1 Introduction

Recently, in order to provide various services in mobile communications, not only voices but also data and images, the demand for broadband multimedia is dramatically increasing. Especially, for effectively overcoming the shadow region of radio propagation in urban and/or crowded in-building areas, radio-over-fiber (ROF) technology using optical fibers is an alternative solution demonstrated to support fused wireline–wireless transmission systems [1–5]. Application systems using ROF consist of central station (CS) and remote base station (RBS), which is interconnected by optical fibers as a channel medium of transmitting radio frequency (rf) band signals. Receivers in the RBS recover the transmitted signals and then radiate them through the air by antenna. Thus, ROF technology could centralize expensive switching systems and modulator/demodulator equipment independently, existing for each base station and the following interfaces as well so that CS makes it possible to adaptively control the services and capacity in specific local areas providing customers of diverse demands. In addition, low cost and ease of maintenance are the expected advantages due to the complete communication systems implemented by establishing terminal units and transmitters/receivers just in CS and RBS simply organized by containing broadband antenna units.

Furthermore, complex-coupled distributed feedback (DFB) lasers, including gain-coupled and loss-coupled ones, have been considered as promising transmitter sources for the long-wavelength optical communications because of higher single mode yield, better stabilized output power, and lasing wavelength compared with those of index-coupled laser diodes (LD) [6, 7]. One of the complex-coupled DFB LD is gain-coupled one, using periodic gain change in active layer itself. We refer this as "gain grating" by an adjacent anti-phase index grating to obtain gain coupling without index coupling and avoiding absorption in the corrugated region [8]. It has, however, disadvantages in yields and reliability associated with complicated fabrication processes of active layer etching and overgrowth. On the other hand, loss-coupled device employs periodic light intensity change by using an absorptive medium, so that it has simpler process and more reliable characteristics than those of the gain-coupled LDs. (We classified the complex-coupled DFB lasers in gain- and loss-coupled DFB's for convenience even though they are in the category of gain-coupled device with introducing slightly different mechanisms.) This is due to the introduction of diffraction grating on an absorptive layer within the corrugation region. Therefore, we call this configuration as an "absorptive or loss grating". Detailed physics of both DFB mechanisms are described in [9, 10]. Since an additional growth step for insertion of an absorption medium in the grating is required, the fabrication process of the loss-coupled LD, therefore, has additive process compared to that of an index-coupled device [11].

In this work, we demonstrate the fabrication and characterization for microwave optical links of a loss-coupled 1550 nm DFB laser diode incorporating an automatically buried absorptive InAsP layer in DFB LD fabrication which reduces process steps compared to the conventional loss-coupled LD. Measured intermodulation distortion terms for the evaluation of fabricated transmitter source device of the ROF links as well as the electro-optical conversion and frequency responses are explored for the DFB laser of loss-coupled mechanism with a reduced step growth.

2 Structure and fabrication

Structure of the fabricated loss-coupled 1550 nm DFB laser diode is shown in Fig. 1. It has a 1% compressive strained multi-quantum well (MQW) of five wells and the first order grating formed by a chemical etching through a laser holographic photolithography on InP substrate. To

✉ Fax: 1-410-516-5566, E-mail: jhan16@jhu.edu

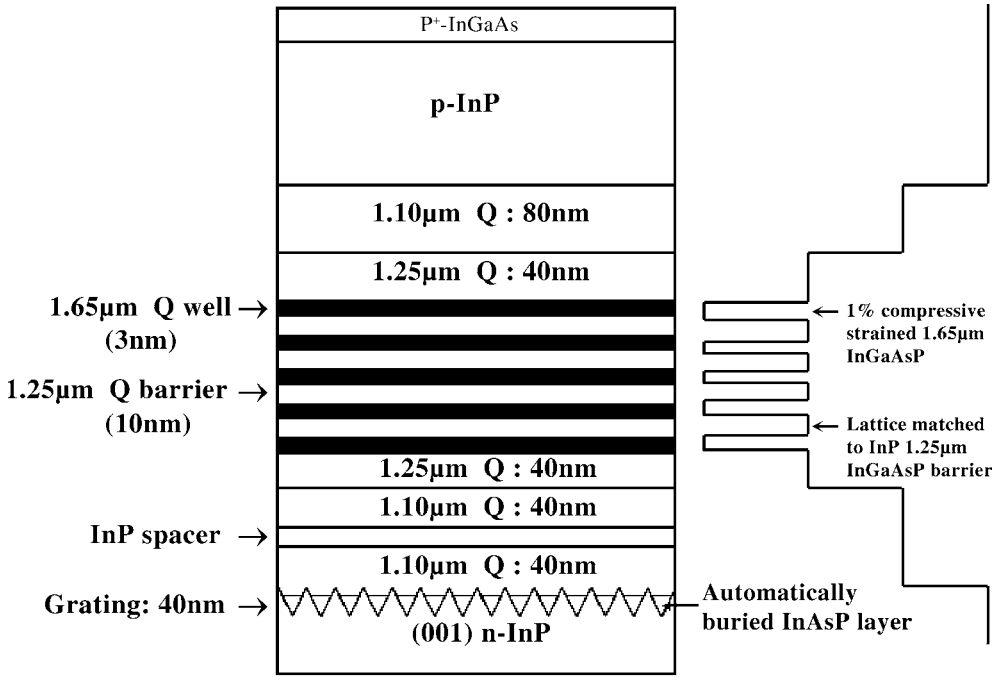

FIGURE 1 Structure of fabricated 1550 nm DFB laser with automatically buried InAsP layer

implement a loss-coupled mechanism of DFB lasers, an automatically buried absorptive InAsP layer was grown between the valley of a corrugated InP and an InGaAsP layer (1.10 μm) by introducing a new overgrowth method reported in previous study [12]. As shown in Fig. 1, an InP spacer was inserted inside the InGaAsP layer (1.10 μm). This structure effectively improves the coupling constant (κ) as well as the quality of the MQW grown above it. Improvement in the coupling constant can be achieved by placing a lower InGaAsP layer (1.10 μm) directly on top of the absorptive InAsP one. The InP spacer grown on top of the lower InGaAsP layer plays a role in planarizing corrugations and reducing defects caused by the interface between the grating and the lower InGaAsP layer. Thickness of the InP spacer layer has to be precisely optimized to reduce the defects originating from the interface between the InAsP and the InGaAsP layers as well as to keep the κ value large. Planar buried heterostructure (PBH) type DFB LDs having width of emission region of 1.5 μm and cavity length (L) of 300 μm were fabricated. Anti-reflective (3%) and highly reflective (95%) coating processes were performed. The coupling constant was estimated to be about 60 cm^{-1}. Details of epitaxial layer growth and device fabrication process were described in [12, 13].

3 Results and discussion

Light–current (L–I) characteristics curve of the fabricated laser diode is in Fig. 2a measured after pig-tailing the transistor outline (TO) can LD package. The threshold current (I_{th}) is 5.5 mA and the slope efficiency (SE) is 0.11 mW/mA where the first order differentiation of L–I curve is directly the curve of SE. Figure 2b is the electrical frequency response of the pig-tailed LD, according to the in-

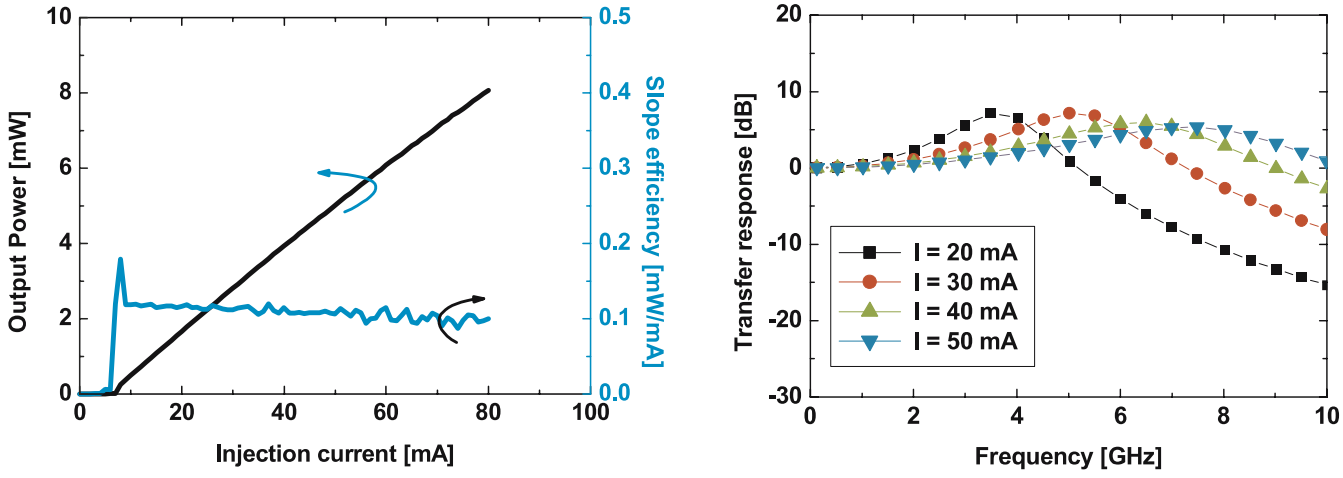

FIGURE 2 Characteristics of laser diode: (**a**) Light–current response; (**b**) frequency response

jected current to the LD. The resonance frequency gradually increases for more than 6 GHz following the drive current up to 50 mA. (According to the following further measurement, this frequency response curve is almost the same when the operating current is larger than 50 mA.)

Measurement for the intermodulation distortion is performed as the setup shown in Fig. 3 where the two-tone test is carried out in personal communication system (PCS) 1.8 GHz frequency bands. The two sinusoidal signals independently generated from signal generators with separation of 1 MHz and equally 0 dBm in mean powers (or 1 mW) are coupled by a combiner directly injected to the laser diode after ac coupling by a capacitor for removing dc noises. The dc bias or the injection current was controlled by a current generator for driving the LD. The LD is optically isolated for one direction by inserting an optical isolator when it was fiber pig-tailed. FC/APC optical connectors prevent distortion due to the reflections in the interfaces of components and fibers; connect the modulated light source and the photodetector module (PD) directly. Electrical spectrum analyzer measures third order intermodulation distortion terms (IMD_3) from the induced photocurrent.

In Fig. 4, as a result, IMD_3 is enhanced monotonously from −50 dBc to −65 dBc up to operating current of 50 mA or mean power of 5 mW where the maximum IMD_3 swing was ±0.5 dB. This result is comparable to those of the previous report at 1.8 GHz [14, 15], where we achieved DFB laser of loss coupling mechanism in simpler process by the automatically buried absorptive layer. The results of third-order intermodulation distortion show that the IMD_3 decreases as the injection current to the laser increases, which could be estimated from reduced modulation depth (m) as the optical output power of laser diode increases with the constant rf signal power from the following expressions,

$$P = \bar{P} + \frac{\partial P}{\partial I}\left(I - \bar{I}\right) + \frac{1}{2}\frac{\partial^2 P}{\partial I^2}\left(I - \bar{I}\right)^2 + \frac{1}{6}\frac{\partial^3 P}{\partial I^3}\left(I - \bar{I}\right)^3 + \ldots \quad (1)$$

$$P = \bar{P} + \hat{P}\left[\cos(\omega_1 t) + \cos(\omega_2 t)\right] = \bar{P}\left[1 + m\left(\cos(\omega_1 t) + \cos(\omega_2 t)\right)\right] \quad (2)$$

$$m = \frac{\hat{P}}{\bar{P}} \quad (3)$$

where, P is the total output modulated optical power in Taylor series (1) or in sinusoidal form (2), the average optical power of $\bar{P}$; the two-tone frequencies, ω_1 and ω_2 with equal amplitude $\hat{P}$ (average rf input power is $\frac{\hat{P}}{2}$); m defined as the modulation depth which is a ratio of rf peak power and optical power; I is the injected current; $\overline{I}$ is the LD threshold current.

However, when the operating current is larger than 50 mA (or 5 mW of optical power), this value keeps almost constant with little enhancement. Due to the deteriorated light–current characteristics (Fig. 2), the smaller modulation depth does not assure better IMD_3 term. It degrades the intermodulation because of the increased non-linear factors included in those light–current characteristics at high current or high output powers. Furthermore, as the power increases the IMD fluctuation follows the similar tendency to be increased up to ±2 dB. When above 5 mW or 50 mA, the IMD oscillation was stable in ±0.5 dB. This phenomenon is resulted from the junction temperature induced from thermal impedance of semiconductor laser diode [16]. Lasers are thermally unstable unless they reach the temperature they could maximally increase according to their own thermal impedance. Thus, this was verified from the thermal equilibrium that the fluctuation reduced after operating one hour more that it became steady to be less than ±0.5 dB.

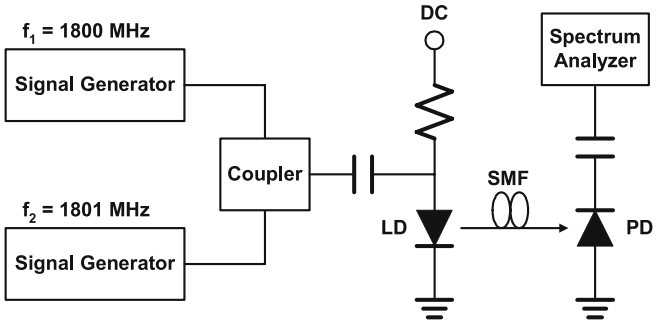

FIGURE 3 Two-tone test experimental setup for intermodulation distortion measurement

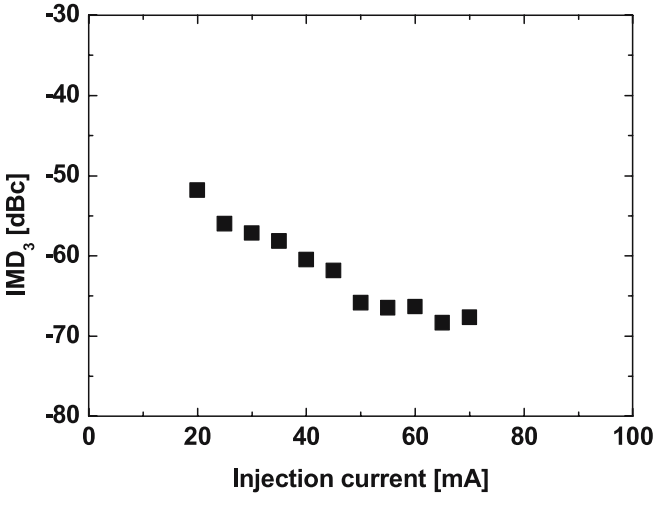

FIGURE 4 Measured result of third-order intermodulation distortion

4 Summary and conclusion

The application of loss-coupled 1550 nm distributed feedback laser diode with automatically buried absorptive layer for the microwave optical fiber network was demonstrated. This absorptive layer for the loss-coupled laser implemented by a single step growth that simplifies device fabrication steps compared to those of conventional loss-coupled devices. It showed linearity up to 5 mW (or 50 mA) with slope efficiency of 0.11 mW/mA and third order intermodulation distortion of less than −65 dBc for 1800 MHz and 1801 MHz frequencies. Intermodulation distortion was gradually improved according to the increased driving current or optical power due to the decreased modulation depth under small deteriorations of light–current response linearity and thermal stability.

REFERENCES

1 H.-H. Lu, Y.-C. Lin, Y.-H. Su, H.-S. Su, IEEE Photon. Technol. Lett. **16**, 251 (2004)
2 H.-H. Lu, P.-C. Lai, W.-S. Tsai, IEEE Photon. Technol. Lett. **16**, 1215 (2004)
3 C. Lim, A. Nirmalathas, M. Attygalle, D. Novak, R. Waterhouse, J. Lightwave Technol. **21**, 2203 (2003)
4 A. Kaszubowska, L.P. Barry, P. Anandarajah, IEEE Photon. Technol. Lett. **15**, 852 (2003)
5 C. Carlsson, H. Martinsson, R. Schatz, J. Halonen, A. Larsson, J. Lightwave Technol. **20**, 1740 (2002)
6 K. David, G. Morthier, P. Vankwikelberge, R.G. Baets, T. Wolf, B. Borchert, IEEE J. Quantum Electron. **QE-27**, 1714 (1991)
7 G.P. Li, T. Makino, R. Moore, N. Puetz, K.-W. Leong, H. Lu, IEEE J. Quantum Electron. **QE-29**, 1736 (1993)
8 Y. Nakano, H.-L. Cao, K. Tada, Y. Luo, M. Dobashi, H. Hosomatsu, Jpn. J. Appl. Phys. **32**, 825 (1993)
9 J. Hong, H. Kim, T. Makino, IEEE J. Lightwave Technol. **16**, 1323 (1998)
10 C. Gourgon, J. Robadey, D. Martin, F. Filipowitz, L. Mahler, N.H. Ky, D. Deveaud, F.K. Reinhart, IEEE Photon. Technol. Lett. **12**, 765 (2000)
11 Y. Inaba, H. Nakayama, M. Kito, M. Ishino, K. Itoh, IEEE J. Sel. Top. Quantum Electron. **7**, 152 (2001)
12 S.W. Park, C.K. Moon, J.H. Kang, Y.K. Kim, E.H. Hwang, B.J. Koo, D.Y. Kim, J.-I. Song, J. Cryst. Growth **258**, 26 (2003)
13 S.W. Park, C.K. Moon, J.C. Han, J. -I. Song, IEEE Photon. Technol. Lett. **16**, 1426 (2004)
14 A.J. Lowery, D. Novak, IEEE J. Quantum Electron. **QE-30**, 2051 (1994)
15 J. Chen, R.J. Ram, R. Helkey, IEEE J. Quantum Electron. **QE-35**, 1231 (1999)
16 J.-H. Han, S.W. Park, IEEE Trans. Dev. Mater. Reliab. **4**, 292 (2004)